

Remarks

The various parts of the Office Action are discussed below under related headings.

Claim Rejection - 35 USC § 101

Claim 13 was rejected as being directed to non-statutory subject matter. This rejection is now moot in that claim 13 has been amended to recite subject matter that clearly is statutory.

Objection to Specification and Claim Rejection - 35 USC § 112, 1st ¶

The specification was objected to¹ and claims 7 and 9-14 were rejected for want of an enabling disclosure. According to the Examiner, the specific process for automatic data fusion and updating are not taught in the specification. Indeed, the specification does not describe at length such a process as the same was known in the art at the time the application was filed. Automatic image fusion programs existed and were available to persons skilled in the art at the time the application was filed. In view of this, it is respectfully submitted the application is enabling. Therefore, the objection to the specification and rejection of claims 7 and 9-14 should be withdrawn.

Claim Rejection - 35 USC § 112, 2nd ¶

The claims were rejected as being indefinite for several reasons. The Examiner's comments have been considered and the claims amended to remove any issue as to indefiniteness. Accordingly, the rejection should be withdrawn.

Claim Rejections - 35 USC § 103

The Examiner has rejected the claims as being unpatentable over Swerdloff U.S. Patent No. 5,661,773 taken alone or in combination with WO 97/40766. As will become apparent from the following discussion, the Swerdloff patent teaches a method that is fundamentally different from the claimed method.

As understood, Swerdloff somehow makes a treatment plan and then carries out that treatment. During the treatment, radiation errors are determined and then, based upon the determined errors, a next treatment is planned.

¹ In the statement of the objection the Examiner referred to claim 1 but it appears that the Examiner intended to refer to claim 7.

Applicants' method as set forth in the claims involves producing or updating an inversely planned radiotherapy plan. The claimed method does not rely on the result of the actual treatment. Instead, applicants' method as claimed assumes the dose distribution has been set sufficiently good in the first inverse plan, and then calculates a new plan on the basis of the planned results of the first plan. The new up-to-date plan is adapted, for example, to new CT-data. Applicants' claimed method does not require a determination to be made of any errors that may have occurred during the earlier treatment.

That is, Swerdloff bases his second plan upon determined errors in the first plan while the applicants' method as claimed does not require determination of such errors but instead saves a lot of effort and time by reusing the planning data of the first plan instead of newly establishing another plan from scratch. The second plan is adapted from the first plan by taking into account, for example, organ shifts as determined by a new CT-scan. Swerdloff does not trust his original plan. Instead, it is assumed that errors will occur and Swerdloff seeks to correct these errors by building a completely new plan, which is exactly the effort the present invention avoids. In this regard, the Examiner's attention is directed to column 3, lines 57 to 61 of the Swerdloff patent, which reads:

Where a treatment error (i.e. over or under radiation) has occurred, the error can be noted using the human interface and can be used to alter desired dose maps during later therapy sessions to compensate for the errors.

Also, in column 2, lines 51 to 63, it is said:

After different irradiation zones within a tomographic image have been identified, the interface allows the operator to specify various radiation doses for each irradiation zone, to run a test simulation which takes into account radiation scatter during a therapy session to derive a theoretical pre-radiation dose map based on the doses specified by the operator, to easily change the doses specified by the operator as a function of the theoretical pre-radiation dose map that results, to verify radiation dose after a therapy session, and to plan for subsequent therapy sessions based on dose delivered during previous therapy sessions.

The last part, namely "to plan for subsequent therapy sessions based on dose delivered during previous therapy sessions," confirms that such technique is intended to take into account the actually applied dose (i.e. the error therein) for future planning.

Moreover, dosage-volume histograms, the basis for the planning according to the present invention as claimed, are nowhere mentioned in the Swerdloff patent. For this additional reason, Swerdloff does not fairly teach or suggest applicants' invention as claimed.

WO 97/40766 does not overcome above-noted fundamental deficiencies of the Swerdloff reference as a teaching reference vis-a-vis the claimed subject matter. Thus, the applied references, taken alone or together, do not lead the skilled person to applicants' method as set forth in the claims.

As a final item, the Examiner, on the PTO-1449 form listing the art cited in the International Search Report, indicated consideration of four of the documents that were submitted. However, the Examiner drew a line through DE 199 12 708 for an unknown reason. The Examiner did write something in the margin, but it was partly cut off on the copy attached to the Office Action. The Examiner is requested to clarify why the German patent document was crossed off. It is noted that the relevance of the German patent document is indicated in the European Search Report, a duplicate copy of which is attached. In particular, the German patent document was cited as being of general background interest in respect of claims 4 and 7, with specific reference being made to column 3, lines 18-27, and column 4, lines 17-38.

This application is now believed to be in condition for allowance and an early action to that effect is earnestly solicited.

Respectfully submitted,

RENNER, OTTO, BOISSELLE & SKLAR, LLP

By 

Don W. Bulson, Reg. No. 28,192

1621 Euclid Avenue
Nineteenth Floor
Cleveland, Ohio 44115
(216) 621-1113

**A. Clean Version of Replacement Paragraph/Section/Claim
with Instructions for Entry**

Please amend the application as follows:

In the Claims:

Please substitute the following amended claims for those of the same number that are presently pending:

1. A method for producing or updating an inversely planned radiotherapy plan for fractionated radiation exposure of a patient, characterised in that an up-to-date radiotherapy plan is calculated at least partly on the basis of the results of an already existing, approved, older plan.
2. The method as set forth in claim 1, wherein pre-set values for calculating the inverse radiotherapy plan are determined from the results of a previously calculated plan.
3. The method as set forth in claim 1, wherein the patient is subject to an imaging method more than once over the duration of fractionated radiation exposure.
4. The method as set forth in claim 1, wherein the patient is subject to an imaging method before each radiotherapy session, wherein only a specified, defined area comprising the target volume is detected.
5. The method as set forth in claim 3, wherein the position of the patient relative to the imaging device is detected outside the region of the patient being imaged by the imaging device by the use of locating markers.
6. The method as set forth in claim 5, wherein the system for locating the markings is calibrated relative to the imaging device, such that the position of the markers can be determined relative to a data set recorded by the imaging device.

10. The method as set forth in claim 9, wherein the information to be adopted into the new plan is transferred by means of a three-dimensional fusion of the contours, drawn in by hand, onto the layers or voxels of a new data set.

12. The method as set forth in claim 9, wherein an image detection plane of an imaging device, with the aid of which the planning data set is to be updated, is determined in an image recording range by introducing a calibration phantom comprising markings which can be detected both by image detection and by an external tracking system, wherein a spatial relationship with the patient markings which are not detected by image detection is produced for the images detected.

13. A computer programmed to perform the method set forth in claim 1.

14. A computer program storage medium comprising a program which, when running on a computer, performs the method set forth in claim 1.

Please add the following new claim:

15. The method as set forth in claim 3, wherein the imaging method is a CT or MR image recording method.

8. The method as set forth in claim 1, wherein the difference between the results of a new radiotherapy plan as compared to a previous plan are automatically quantified and, if the difference is within a previously specified tolerance range, the new plan is automatically qualified as an approved plan.

9. The method as set forth in claim 1, wherein, for transferring a radiotherapy plan onto a more recent planning data set, the position and form of a target volume and the organs to be protected are fully or partly adopted automatically into the new plan from the old plan.

10. (Amended) The method as set forth in claim 9, wherein the information to be adopted into the new [planning data set] plan is transferred by means of a three-dimensional fusion of the contours, drawn in by hand, onto the layers or voxels of [the] a new data set.

11. The method as set forth in claim 10, wherein fusion involves a graphic elastic morphing method of the information to be fused.

12. (Twice Amended) The method as set forth in claim 9, wherein an image detection plane of an imaging device, with the aid of which the planning data set is to be updated, is determined in [the] an image recording range by introducing a calibration phantom comprising markings which can be detected both by image detection and by an external tracking system, wherein a spatial relationship with the patient markings which are not detected by image detection is produced for the images detected.

13. (Twice Amended) A [program which, when running on a] computer [or loaded in a computer, causes the computer] programmed to perform the method [in accordance with] set forth in claim 1.

14. (Amended) A computer program storage medium comprising [the] a program [in accordance with claim 13] which, when running on a computer, performs the method set forth in claim 1.

New claims:

15. The method as set forth in claim 3, wherein the imaging method is a CT or MR image recording method.

EXHIBIT

Tables*

From: Advanced Monte Carlo for Radiation Physics, Particle Transport Simulation and Applications: Proceedings of the Monte Carlo 2000 Conference, Lisbon, 23-26 October, 2000. Springer, Berlin, 2001
Eds A Kling, F Barao, M. Nakagawa, L. Travora and P. Vaz

Inverse Treatment Planning for Radiation Therapy Based on Fast Monte Carlo Dose Calculation

M. Fippel¹, M. Alber¹, M. Birkner¹, W. Laub¹, F. Nüsslin¹, and I. Kawrakow²

¹ Radiologische Universitätsklinik Tübingen, Germany

² Institute for National Measurement Standards Ottawa, Canada

Abstract. An inverse treatment planning system based on fast Monte Carlo (MC) dose calculation is presented. It allows optimisation of intensity modulated dose distributions in 15 to 60 minutes on present day personal computers. If a multi-processor machine is available, parallel simulation of particle histories is also possible, leading to further calculation time reductions. The optimisation process is divided into two stages. The first stage results in fluence profiles based on pencil beam (PB) dose calculation. The second stage starts with MC verification and post-optimisation of the PB dose and fluence distributions.

Because of the potential to accurately model beam modifiers, MC based inverse planning systems are able to optimise compensator thicknesses and leaf trajectories instead of intensity profiles only. The corresponding techniques, whose implementation is the subject for future work, are also presented here.

1 Introduction

Inverse or optimised treatment planning becomes more and more important especially for intensity modulated radiation therapy (IMRT). Iterative optimisation algorithms provide primary fluence profiles based on given treatment objectives (motivated by physical [1] and/or biological assumptions [2]) and dose calculation methods. Monte Carlo (MC) dose calculation [3] will be the preference in future because of the potential to accurately model treatment machines as well as photon and electron transport in heterogeneous human tissue [4-6]. Computation time will be irrelevant in future because of the rapidly increasing CPU speed and the development of optimised MC codes designed for the material and energy range of radiation therapy, e.g. the X-ray Voxel Monte Carlo [7-9] (XVMC) algorithm. XVMC is coded in C++ and allows parallel computation of particle histories on multiple processor units. Special combinations of variance reduction techniques like photon splitting, electron history repetition and Russian Roulette allow the calculation of dose distributions within minutes or seconds for photon respectively electron beams.

For the present investigation the XVMC code has been integrated into "Hyperion" [10], an IMRT planning system based on constrained biological optimisation and a gradient method to calculate the primary fluence updates. The treatment planning starts with the definition of critical organ structures and corresponding maximum damages measured by an effective dose. The implemented

optimisation algorithm tries to maximise the dose (or damage) in the tumor volume by retaining the organ constraints, which can be changed by the user during the planning process.

2 Monte Carlo Optimisation Procedure

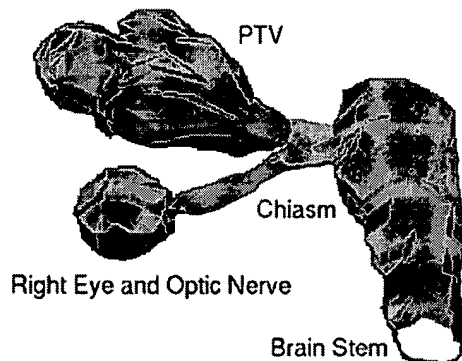


Fig. 1. Beam's eye view of one of the four 6 MV photon beams to irradiate a optical nerve carcinoma. PTV means planning target volume and denotes the tumor region

The first IMRT optimisation stage employs a finite size pencil beam (PB) algorithm for calculating the dose distribution and the objective function derivatives with respect to the primary fluence elements. The second stage starts with MC verification ($D_{MC}^0(r)$) of the PB dose distribution ($D_{PB}(r)$). Differences between $D_{MC}^0(r)$ and $D_{PB}(r)$ are subject to further optimisation, but this time employing XVMC for dose calculation. To obtain the fluence updates for the next iteration step we have to know the dose contribution $T(i, r)$ of each beam element i . In principle, it is possible to compute these values also by Monte Carlo. However, the function $T(i, r)$ is frequently used and the storage and calculation time requirements are huge. Therefore, to differentiate the objective function we still use $T_{PB}(i, r)$ of the PB algorithm. The convergence of this approach is still unproven, but it could be shown that there are problem dependent (heterogeneity of the treatment volume, beam parameters, objective function) convergence conditions [6].

During each iteration step the fluence updates are transformed into corresponding initial particles with positive or negative statistical weights. Positive weight particles increase and negative weight particles decrease the dose along their trajectory. This procedure corrects the dose distribution $D_{MC}^k(r)$ of the previous step k due to the fluence of the present step. Additionally, the statistical fluctuations are smaller for the new distribution $D_{MC}^{k+1}(r)$. The optimisation ends if the objective function changes are smaller than a user provided value.

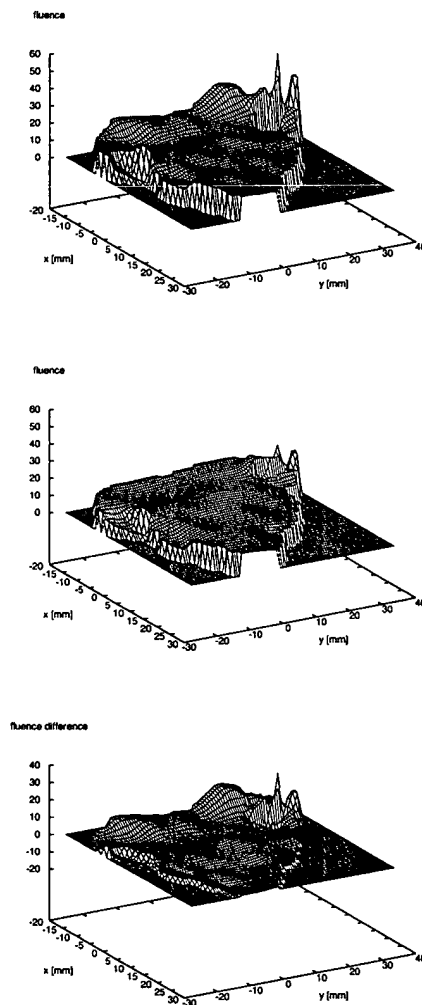


Fig. 2. The intensity profile of the beam from Fig. 1 after PB and MC optimisation (upper plot), PB optimisation only (central plot) and the difference between both distributions (lower plot)

As an example we simulated the treatment of a carcinoma near the right eye and optical nerve. In this region we find large density variations (soft tissue, bone, air). Therefore, the quality of dose calculation will have significant influence on

the resulting intensity profiles. For the treatment of this patient four beams of 6 MV photon energy have been arranged with different directions. Figure 1 shows one beam's eye view of the tumor (PTV = planning target volume) and the critical structures. In Fig. 2 the fluence profiles of this beam after optimisation with Monte Carlo (upper plot) and pencil beam dose calculation (central plot) are represented. The lower plot shows the fluence difference between the MC and PB profiles which are in the order of 50% especially in the third quadrant. There, the MC algorithm has to compensate for lateral electron scatter by increasing the primary photon fluence. A pencil beam algorithm, however, is not able to model electron transport correctly. Therefore, the corresponding profile is too flat.

3 Beam Modifiers

Beam modifiers like multi-leaf collimators (MLC) or compensators can be integrated directly into the optimisation procedure and to the MC simulation by retaining the fluence update approach. In the following we will explain the corresponding techniques, which will be implemented into "Hyperion".

3.1 Compensators

Intensity modulated beams can be generated by inserting a compensator into the beam line. Generally, a compensator is a block of lead with varying thickness d leading to variable attenuation and photon fluence. Usually, the result of "conventional" IMRT planning systems are fluence profiles. After finishing the iteration procedure, these profiles are converted into compensator shapes. However, the compensator produces additional photon scatter and electron contamination, which should be taken into account by the optimisation process. Only Monte Carlo algorithms are able to model compensators correctly. Therefore, MC based IMRT planning systems should optimise compensator shape and thickness rather than fluence profiles.

Assume that after the iteration k the compensator thickness at a definite location is $d^k(x, y)$ (x and y denote the coordinates within the compensator system). After the next iteration ($k + 1$) the compensator thickness changes to $d^{k+1}(x, y)$, which can be larger, smaller, or equal to $d^k(x, y)$. A photon hitting the compensator may be absorbed by the compensator material or it survives with or without scattering. This depends on the sampled free photon path length. Furthermore, Compton, pair and photo electrons (positrons) and additional bremsstrahlung photons can be produced. To calculate the dose update for iteration $k + 1$, we perform the following steps repeatedly, if $d^k(x, y)$ and $d^{k+1}(x, y)$ differ for the given beam element:

- Take an initial photon from the fluence distribution above the compensator.
- For $d^k(x, y)$ and $d^{k+1}(x, y)$ sample the particle states behind the compensator using identical random numbers.

- If the states are identical, do nothing.
- If the states are different, simulate the first photon history (k) in the patient volume using a negative weight and the second photon history ($k + 1$) using a positive weight.
- The corresponding history simulation is unnecessary, if one of the photons is absorbed by the compensator completely, i.e. also the secondary particles of this history are absorbed.
- Take the next photon from the fluence distribution above the compensator, etc.

Secondary electrons produced within the compensator can be rejected if their energy is too small to reach the patient surface (range rejection). On the other hand, electrons arising from the compensator's bottom side must be simulated because of their additional patient dose contribution (electron contamination).

3.2 Dynamic Multi Leaf Collimators

An alternative method to deliver intensity modulated beam profiles in radiation therapy is the use of dynamic multi-leaf collimators (DMLC). The Monte Carlo implementation of DMLCs is comparable to the compensator case. If the positions are given by a set of time dependent functions $x_l(t)$ (l denotes the leaf number and x stands for all geometrical parameters necessary to model the leaf position), continuous leaf motion can be simulated by choosing the time t randomly from a uniform distribution. Therefore, the IMRT planning system should be able to find the optimum by iterating a sequence of leaf trajectories $x_l^k(t)$ similar to the sequence of compensator thicknesses $d^k(x, y)$ (see Sec. 3.1).

4 Conclusion

The new system allows MC optimisation of IMRT dose distributions in 15 to 60 minutes on present day personal computers. If a multi-processor machine is available, the calculation time can be reduced further. Therefore, it is a practical tool improving the treatment of cancer. Especially for the modelling of beam modifiers (compensators, MLC) and in regions with large density variations (lung, head and neck) the benefit of MC algorithms compared to conventional dose determination is indispensable.

References

1. A. Brahme, J. E. Roos, I. Lax: Phys. Med. Biol. **27**, 1221 (1982)
2. M. Alber, F. Nüsslin: Phys. Med. Biol. **44**, 479 (1999)
3. W. R. Nelson, H. Hirayama, D. W. O. Rogers: *The EGS4 code system*, SLAC Report **265** (1985)
4. R. Jeraj, P. Keall: Phys. Med. Biol. **44**, 1885 (1999)
5. L. Bogner, J. Scherer, M. Herbst: *Physica Medica* **15**, 111 (1999)

6. W. Laub, M. Alber, M. Birkner, F. Nüsslin: Phys. Med. Biol. **45**, 1741 (2000)
7. I. Kawrakow, M. Fippel, K. Friedrich: Med. Phys. **23**, 445 (1996)
8. M. Fippel: Med. Phys. **26**, 1466 (1999)
9. I. Kawrakow, M. Fippel: Phys. Med. Biol. **45**, 2163 (2000)
10. M. Alber, M. Birkner, W. Laub, F. Nüsslin: 'Hyperion: An integrated IMRT planning tool'. In Proc.: *13th International Conference on the Use of Computers in Radiation Therapy, Heidelberg, Germany, May 23-26, 2000* ed. by W. Schlegel and T. Bortfeld (Springer-Verlag Berlin Heidelberg New York) pp. 46-48

Optimization of importance factors in inverse planning

L Xing, J G Li, S Donaldson, Q T Le and A L Boyer

Department of Radiation Oncology, Stanford University School of Medicine, Stanford, CA 94305-5304, USA

E-mail: lei@reyes.stanford.edu (L Xing)

Received 23 February 1999, in final form 11 June 1999

Abstract. Inverse treatment planning starts with a treatment objective and obtains the solution by optimizing an objective function. The clinical objectives are usually multifaceted and potentially incompatible with one another. A set of importance factors is often incorporated in the objective function to parametrize trade-off strategies and to prioritize the dose conformality in different anatomical structures. Whereas the general formalism remains the same, different sets of importance factors characterize plans of obviously different flavour and thus critically determine the final plan. Up to now, the determination of these parameters has been a ‘guessing’ game based on empirical knowledge because the final dose distribution depends on the parameters in a complex and implicit way. The influence of these parameters is not known until the plan optimization is completed. In order to compromise properly the conflicting requirements of the target and sensitive structures, the parameters are usually adjusted through a trial-and-error process. In this paper, a method to estimate these parameters computationally is proposed and an iterative computer algorithm is described to determine these parameters numerically. The treatment plan selection is done in two steps. First, a set of importance factors are chosen and the corresponding beam parameters (e.g. beam profiles) are optimized under the guidance of a quadratic objective function using an iterative algorithm reported earlier. The ‘optimal’ plan is then evaluated by an additional scoring function. The importance factors in the objective function are accordingly adjusted to improve the ranking of the plan. For every change in the importance factors, the beam parameters need to be re-optimized. This process continues in an iterative fashion until the scoring function is saturated. The algorithm was applied to two clinical cases and the results demonstrated that it has the potential to improve significantly the existing method of inverse planning. It was noticed that near the final solution the plan became insensitive to small variations of the importance factors.

1. Introduction

The purpose of radiation treatment is to deliver a known dose of radiation to diseased tissues while minimizing the dose to normal structures. Conventional 3D conformal radiation therapy is ultimately limited by the fluence profiles of the incident beams, which can only be either open or wedged fields (Starkschall 1992, Ezzell 1996, Xing *et al* 1998a). Significant improvement to the dose distribution can be achieved in many cases by purposely modulating the intensity profiles of the incident photon beams. Intensity modulated radiation therapy (IMRT) using computer controlled multileaf collimators (MLC) is a new modality of radiation therapy and represents the most recent advance in the field (Brahme *et al* 1982, Bortfeld *et al* 1990, Webb 1994, Holmes and Mackie 1994, Xing and Chen 1996, Xing *et al* 1998b, Ling *et al* 1996, Mohan *et al* 1994, Olivera *et al* 1998, Carol *et al* 1997, Lof *et al* 1998, Spirou and Chui 1998, Togane *et al* 1998).

In IMRT planning each incident beam is divided into a few hundred beamlets (the size of the beamlets is frequently 1 cm × 1 cm). The beamlet weights are almost exclusively determined by using computer optimization because the best possible beam profiles are not intuitively obvious given the greatly increased degree of freedom in the system. The optimization is usually realized by using so-called inverse planning, that derives a set of optimized beamlets under the guidance of a therapeutic objective function. In more general terms, for a given system this is an issue of obtaining the optimal input parameters that will produce a desired output. In therapeutic plan optimization, the desired output is specified by a dose to an anatomical structure (or a set of voxels), or dose volume histograms (DVHs) for anatomical structures. Alternatively the treatment outcome is optimized based on biological indices such as the normal tissue complication probability (NTCP) and the tumour control probability (TCP). A given objective function can be optimized using a number of optimization algorithms, such as iterative approaches, simulated annealing and filtered backprojection.

The objective function measures the goodness of a selected plan. Its choice is crucial for therapeutic plan selection. A commonly used function is the quadratic objective function, which is given by

$$F = \frac{1}{N} \sum_{n=1}^N r_\sigma [D_c(n) - D_0(n)]^2 \quad (1)$$

where N is the total number of voxels, r_σ is the importance factor that controls the relative importance of a structure σ , and D_0 and D_c are prescribed and calculated doses respectively. Many other types of phenomenological objective functions have been proposed for therapeutic optimization. In general, they are combinations over contributions from the target and the sensitive structures. The objectives to conform the target volume and to spare the sensitive structures are in competition, and the trade-off strategies are parametrized by the importance factors. The ‘optimal’ solution strongly depends on the values of the importance factors. Different sets of importance factors result in different ‘optimal’ solutions and the choice of these parameters becomes part of a decision-making process. Because the ‘optimal’ dose distribution corresponding to a set of importance factors is not known until the beam profile optimization is done, several manual trial-and-error iterations are often needed to find a set of suitable importance factors for the target and sensitive structures. This process becomes increasingly complicated as the number of sensitive structures involved with the plan increases. In many cases, the determination of the parameters is a ‘guessing’ game based on some empirical knowledge. In order for treatment plan optimization to reach its full potential in clinical practice, it is highly desirable to have a rational, or at least semi-deterministic, approach for determining the importance factors.

Treatment plan selection is a multiobjective decision-making process and the trade-off considerations must assimilate those of the decision-maker. In this paper, we report an effective algorithm for computer optimization of treatment plans with inclusion of the decision-maker’s trade-off strategies. The method was demonstrated by applying it to two clinical cases. The quality assessment based on isodose distribution and DVH analysis suggested that the technique has potential to improve significantly the current techniques for plan optimization. It provided a computationally intelligent counterpart to the empirical selection process of the importance factors. Whereas the study used a quadratic objective function, the concepts and findings have broad implications for treatment plan optimization. The technique can be easily generalized to deal with other types of phenomenological objective functions.

2. Method

2.1. Theoretical considerations

The ideal treatment plan would deliver the prescribed dose to the target volumes uniformly while simultaneously delivering little or no radiation to the adjacent sensitive structures. Since the ideal treatment plan generally is not attainable, each potential plan must make trade-offs in the doses delivered to the target volumes and the sensitive structures. A set of competing plans makes different trade-offs among the various structures involved in the treatment. That is, for a given patient and beam configuration there are many ‘optimal’ solutions corresponding to different sets of importance factors. Further selections in the pool of competing plans are usually based on an empirical judgement (e.g. by visually inspecting the plans). In principle, one can exhaustively compute all plans corresponding to different sets of importance factors and visually select the one that is clinically most sensible. But this approach is computationally inefficient and difficult. For a given patient, it would be useful in practice to be able to come up with a set of $\{r_\sigma\}$ which produces a plan consistent with the planner’s expectation in an ordinary situation. At least this will provide a good starting point for the plan selection process. For this purpose, it is required to have an explicit representation of the complete objective and trade-off strategies sufficient to define a global optimal point. Unfortunately, the quadratic objective function could only be used to score the plans for a given set of $\{r_\sigma\}$. For a physically feasible plan, there are a series of scores depending on the space specified by the given $\{r_\sigma\}$ and the absolute value of equation (1) becomes meaningless when comparing plans in different r -spaces. An additional score function is needed to rank a group of candidate plans corresponding to different sets of importance factors. Since tumour control and organ tolerance can be assessed by the volumetric information of dose distributions, we will heuristically introduce a DVH score function for this purpose.

The score function is a function of the DVH curve, $V_\sigma(D)$, where V_σ is the fractional volume in the structure σ that receives a dose of D or greater. This function is used to score the competing plans corresponding to the different sets of importance factors $\{r_\sigma\}$. The assessment of relative quality for a plan is based on the ‘distance’ from the ideal DVHs. The highest score should result when the calculated DVH matches with the most-desired DVH, $V_{\sigma 0}(D)$, and the score should become worse gradually when the DVH is away from $V_{\sigma 0}(D)$. A simple example of the DVH preference function is

$$G_\sigma(V) = \sum_D \gamma_\sigma [V_\sigma(D) - V_{\sigma 0}(D)]^2 \quad (2)$$

where γ_σ is the corresponding trade-off parameter controlling the relative importance of the DVH of the structure σ and $V_\sigma(D)$ and $V_{\sigma 0}(D)$ are defined above. For a given beam configuration, the most desired target DVH correspond to the ‘optimal’ dose distribution when r_σ for all sensitive structures is set to zero. For simplicity, we usually assume that it corresponds to the DVH of the idealized case of a uniform target dose. The most-desired DVH for a sensitive structure is usually chosen to be the ideal case in which the sensitive structure volumes receiving non-zero dose become vanishingly small. The heuristic score function given by equation (2) can capture the main feature of the clinical decision-making process. It allows us to reach a compromise between the requirements of the target and the sensitive structures. The solution has the property that the DVH of one structure cannot be further improved without seriously sacrificing the DVHs of the others, and *vice versa*. While the DVHs will be used in this study to evaluate plans, other practical evaluation indices, such as the maximum, minimum or average of the tumour dose, or the maximum or average of normal structure doses, could also be used as selection criteria. The point we wish to emphasize here

is that in order to unambiguously determine the $\{r_\sigma\}$, an additional knowledge or decision tool has to be introduced.

A key issue is the quantization of the relative importance of different structures. The importance factors $\{r_\sigma\}$ were incorporated in the quadratic objective function for this purpose. Unfortunately, these parameters are not a good description of the relative importance because in practice the plan depends on them in a very implicit way. We know very vaguely about the relation between r_σ and the final DVHs. All one knows is that one needs to lower r_σ in order to reduce the influence of the dose requirement in the structure σ in the optimization process, or *vice versa*. The influence of $\{r_\sigma\}$ on the final trade-off is not known until the plan is obtained. It becomes simpler to quantify the relative importance in the DVH representation. In other words, the parameters $\{\gamma_\sigma\}$ in the DVH representation provide a better description of the relative importance of different structures. Intuitively, r_σ relate the dose distributions in different structures and to determine them it is necessary to compromise the doses of all relevant voxels. On the other hand, a DVH state is degenerate; there are many possible dose distributions for a given DVH. Much less information is contained in a DVH in comparison with a dose distribution. As a result, it becomes easier to compromise the requirements of different structures in the DVH representation. When the maximum, minimum or average doses are used as ranking quantities, we expect that it will be even easier to predetermine the corresponding parameters characterizing the relative importance of different structures. In general, the higher the degeneracy of the evaluation quantities, the easier to determine the corresponding trade-off parameters. Of course, the information contained in the evaluation indices will be correspondingly reduced. In order to have enough information to assess the final results, we will use a DVH based score function.

In principle, it is possible to optimize the DVH score function with respect to the beamlet weights to find the optimal solution directly from the pool of all physically realizable plans. This approach has two deficiencies. First, by directly optimizing the DVH score function, we lose control over the dose distribution because of the degeneracy of a DVH state. Clinically, we often prefer one solution over others even though they all have the same DVHs. In other words, we need a formalism that does not simply optimize the DVH score function, but also takes into account our prior knowledge. The second deficiency is computational. A direct optimization of the DVH score function requires a calculation in the dose-volume space to obtain the beam profiles. Our previous experience indicated that the convergence of the iterative calculation for beam profile optimization was slow. A large amount of calculation in the dose-volume space were required to obtain the optimal solution using a ray-by-ray iterative algorithm (Togane *et al* 1998), similar to that observed in the optimization of beam weights and wedge filters in 3D treatment planning (Xing *et al* 1998a). The arguments here are also valid for other types of score functions. In the following we develop a two-step optimization algorithm for IMRT plan optimization. The basic idea is to specify our trade-off strategy in the DVH representation and to find the optimal solution (optimal values of $\{r_\sigma\}$ and the corresponding dose distribution) that assimilates the specified relative importance of different structures in the scheme of the quadratic objective function. This allows us to take advantage of the useful features of each scheme.

2.2. Two-step optimization process

In figure 1 we draw a flow chart of the calculation process. In this work, the ray-by-ray iterative algorithm (SIITP) reported by Xing and Chen (1996) and Xing *et al* (1998b) was employed to obtain the 'optimal' beam profiles. The details of the algorithm have been given by Xing and Chen (1996) and Xing *et al* (1998b) and will not be repeated here. From the computational

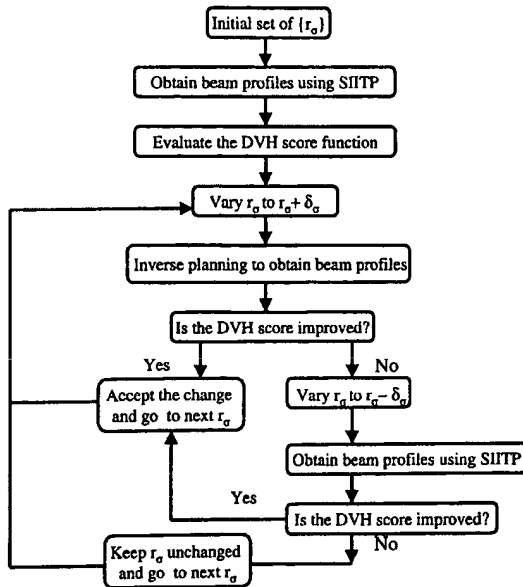


Figure 1. A flow chart of the two-step optimization process.

point of view, the selection procedure of the importance factors $\{r_\sigma\}$ is essentially an additional optimization. That is, it is a process to find a set of $\{r_\sigma\}$ that optimizes the DVH score function (2) with the given trade-off strategy specified by $\{\gamma_\sigma\}$. This is described in the following.

The calculation begins with an initial set of $\{r_\sigma\}$ and the corresponding ‘optimal’ beam profiles. The ‘optimal’ beam profiles are obtained using SITIP. The quality of the plan is then scored by the DVH score function $G_\sigma(V)$ given by equation (2). To proceed, we use Powell’s method of optimization in multidimensions (Press *et al* 1989). The method introduces a series of variations to one of the importance factors r_σ and moves r_σ to the point $r_\sigma + \delta_\sigma$ which minimizes $G_\sigma(V)$ with the remaining r_σ s fixed. The calculation then addresses the next r_σ by repeating the above procedure. The first r_σ will be examined again after all important factors have been addressed. The iteration stops when the change of the DVH score function is less than a pre-chosen precision ϵ ($\epsilon = 0.1\%$ in our calculation). In general, we found that the calculation converges after four to five iterations and the DVH score function saturates to its optimal value. Because the algorithm invokes the beam profile optimization for each variation in r_σ , it is essential to use a fast algorithm for the beam profile calculation.

The above plan optimization was done in two steps. The optimization of equation (1) generates a pool of ‘optimal’ solutions and the DVH score function selects the final solution from the pool of the competing plans. In a sense, the score function acts as a filter to select the final plan from the pool of ‘optimal’ plans corresponding to various sets of $\{r_\sigma\}$. One may also regard the function as an additional soft constraint to the dose distribution in the system.

In our calculation, we usually set the parameter γ_σ to unity for the target and 0.1 to a sensitive structure. Geometrically, in the DVH score function the trade-off parameter γ_σ in equation (2) is related to the relative change in the area under its DVH curve when the DVH of another structure is varied. The above choice implies that the desired change for a sensitive structure is $0.1 \times \delta A$ if the area of the target DVH curve is varied by an amount δA . We found

that this choice mimics the observed clinical trade-off strategy very well. As will be seen in the examples in section 3, this set of $\{\gamma_\sigma\}$ leads to a solution close to what would be considered to be an acceptable solution in an ordinary situation. Only in some special situations (e.g. one or a few sensitive structures can be ignored to improve the dose distribution in other structures) do the values of γ_σ need to be adjusted. Our experience indicates that it is much easier to adjust γ_σ to obtain a sensible plan in comparison with the trial-and-error process to determine $\{r_\sigma\}$.

3. Results and discussion

In section 2 we described an algorithm for importance factor optimization. The approach is based on an additional DVH score function, which utilizes the partial volume information to rank plans corresponding to the different sets of $\{r_\sigma\}$. In this section we will illustrate the theory by studying two clinical cases.

3.1. IMRT plan for a lymphoma involving the right pleura

The above algorithm was first applied to obtain a five-field treatment plan for a lymphoma involving the right pleura. The incident photon energy was 15 MV and the gantry angles of the five incident beams were 10°, 60°, 130°, 210° and 320° respectively. Here the gantry angles were specified using Varian's convention (Varian Medical Systems, Palo Alto, CA). The incident beam directions were obtained based on beam's-eye-view (BEV). The initial importance factors were chosen to be $r_{\text{target}} = 1$, $r_{\text{cord}} = 0$, $r_{\text{right lung}} = 0$ and $r_{\text{left lung}} = 0$ respectively. This choice of importance factors yielded the best dose conformation to the target, but a penalty was paid in that there was no control on the dose delivered to the sensitive structures. The beam profiles corresponding to the initial importance factors were obtained using SIITP. The calculation proceeded with an iterative change of the importance factors, as described in section 1. In the upper row of figure 2 we show the gradual change of the DVHs with the iterative change of the importance factors. As can be expected, the best target DVH was achieved at the beginning of the importance-factor iteration (dashed curves), and the target dose inhomogeneity was increased slightly as the importance factors of the lungs and the spinal cord deviated from zero values. But the sensitive structure DVHs were improved significantly. The final solution (full curves) was a compromise between the requirements of target dose homogeneity and sensitive structure protection.

We found that it took only four to five iterations for the score function to reach the optimum, indicating that the importance factors were weakly correlated. The final solution became increasingly insensitive to small changes of the importance factors in the vicinity of the optimal solution. A small variation (1% to 3%) in one or more importance factors did not cause a noticeable change in the final dose distribution and DVHs. This observation suggested that the final solution was stable. The dotted curves in figure 2 represent the DVHs of the system at the third iteration (the corresponding importance factors are $r_{\text{target}} = 1$, $r_{\text{cord}} = 0.13$, $r_{\text{right lung}} = 0.002$ and $r_{\text{left lung}} = 0.006$). Note that for every new set of importance factors, the beam profiles must be re-optimized using SIITP. The final values of the importance factors were $r_{\text{target}} = 1$, $r_{\text{cord}} = 0.18$, $r_{\text{right lung}} = 0.008$ and $r_{\text{left lung}} = 0.007$ respectively. The final plan was obtained using this set of importance factors to optimize the beam profiles. The score function saturated with further iteration of the importance factors.

The initial 'optimal' isodose distribution of the system on the central axial plane is shown in figure 3(a). The final optimal isodose distribution is shown in figure 3(b). Consistent with the evolution of the DVHs shown in the upper row of figure 2, the doses to the sensitive structures showed significant improvement with the iterative adjustment of the importance

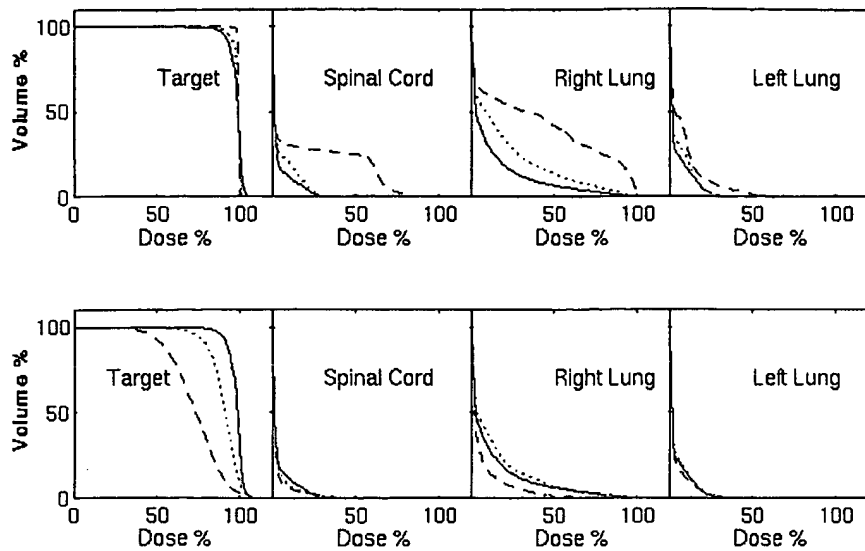


Figure 2. Systematic improvement of the DVHs with the iteration of the importance factors (IMs). The DVHs initially optimized using starting values of the IMs are plotted as dashed lines in the top three figures were $r_{\text{target}} = 1$, $r_{\text{cord}} = 0$, $r_{\text{right lung}} = 0$, and $r_{\text{left lung}} = 0$. The algorithm autoadjusted the importance factors and found the optimal DVHs (full curves). The final IMs were found to be $r_{\text{target}} = 1.0$, $r_{\text{cord}} = 0.18$, $r_{\text{right lung}} = 0.008$ and $r_{\text{left lung}} = 0.007$ respectively. The dotted curves are the 'optimal' DVHs computed in the third iteration ($r_{\text{target}} = 1$, $r_{\text{cord}} = 0.13$, $r_{\text{right lung}} = 0.002$ and $r_{\text{left lung}} = 0.006$). The bottom three figures showed the gradual improvement of the DVHs when the initial importance factors were set to be $r_{\text{target}} = 1$, $r_{\text{cord}} = 0.2$, $r_{\text{right lung}} = 0.2$ and $r_{\text{left lung}} = 0.2$ (dashed curves). The optimal DVHs (full curves) converged to the same solution.

factors. Further improvement in the sensitive structures could not be achieved without seriously sacrificing the target dose homogeneity.

The behaviour of the system when a different set of initial importance factors ($r_{\text{target}} = 1$, $r_{\text{cord}} = 0.2$, $r_{\text{right lung}} = 0.2$ and $r_{\text{left lung}} = 0.24$ respectively) was used is shown in the bottom row of figure 2. In this case, the target DVH was improved gradually as the importance factor iteration proceeded and the DVHs of the sensitive structures were compromised in order to gain target dose conformation. The importance factors corresponding to an intermediate state (the dotted curves) were $r_{\text{target}} = 1$, $r_{\text{cord}} = 0.18$, $r_{\text{right lung}} = 0.01$ and $r_{\text{left lung}} = 0.12$ respectively. The system converged to the same DVHs and isodose distribution.

3.2. Four-field IMRT treatment of a lymphoma involving the right orbit

We now discuss the optimization of a four-field boost plan for a lymphoma involving the right orbit. The incident photon energy was 6 MV and the gantry angles of the four incident beams were 0° , 45° , 90° and 135° . The gantry angles were selected on the basis of BEV and no attempt was made to fine-tune the beam orientations. A small dose grid, 0.25 cm, was used in this calculation to accommodate the relatively small anatomical structures in this case.

A few initial sets of importance factors were tested. In figure 4(a) we show a systematic improvement in the target and sensitive structure DVHs as the iteration of the importance

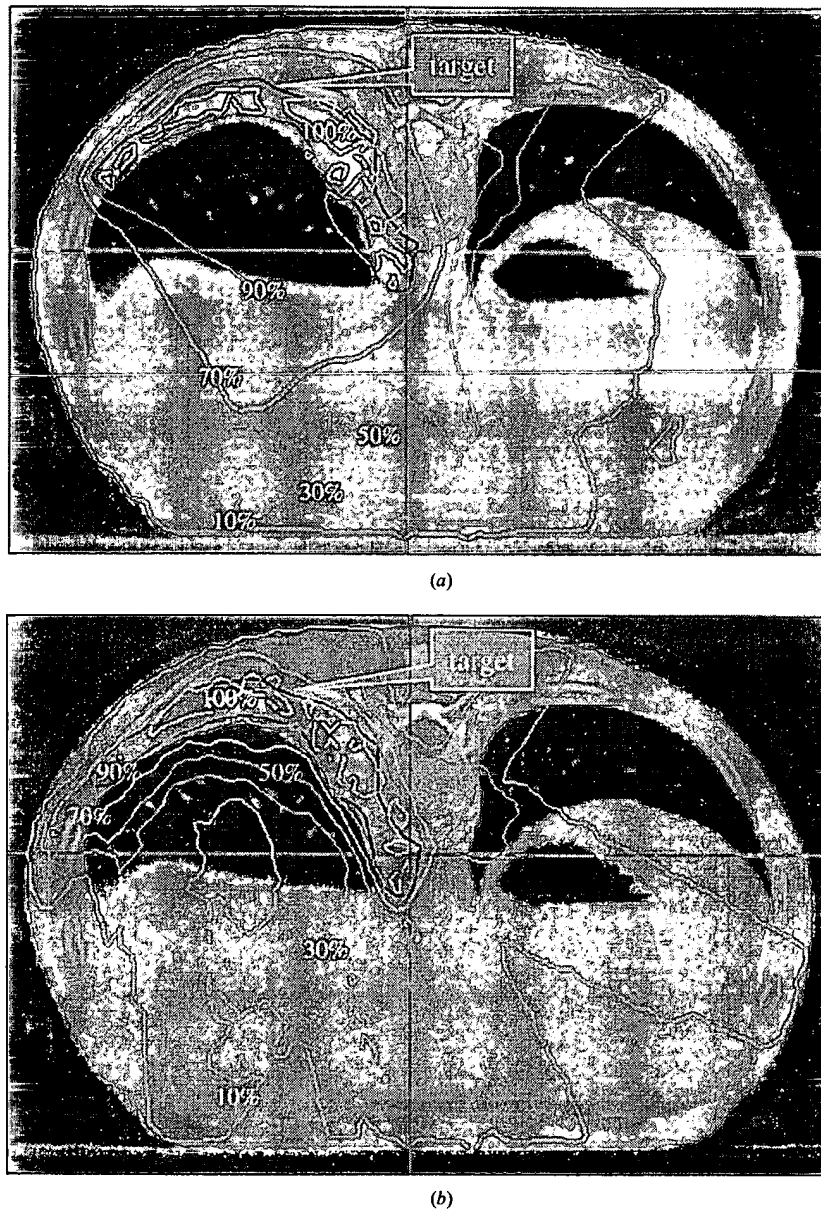


Figure 3. Axial isodose distributions corresponding to the initial set and the final set of importance factors for a five-field IMRT treatment plan for a lymphoma involving the right pleura.

factors proceeds. The initial value of importance factors for the target was set to unity and those for other sensitive structures were set to zero. Once again, five iterations were all that

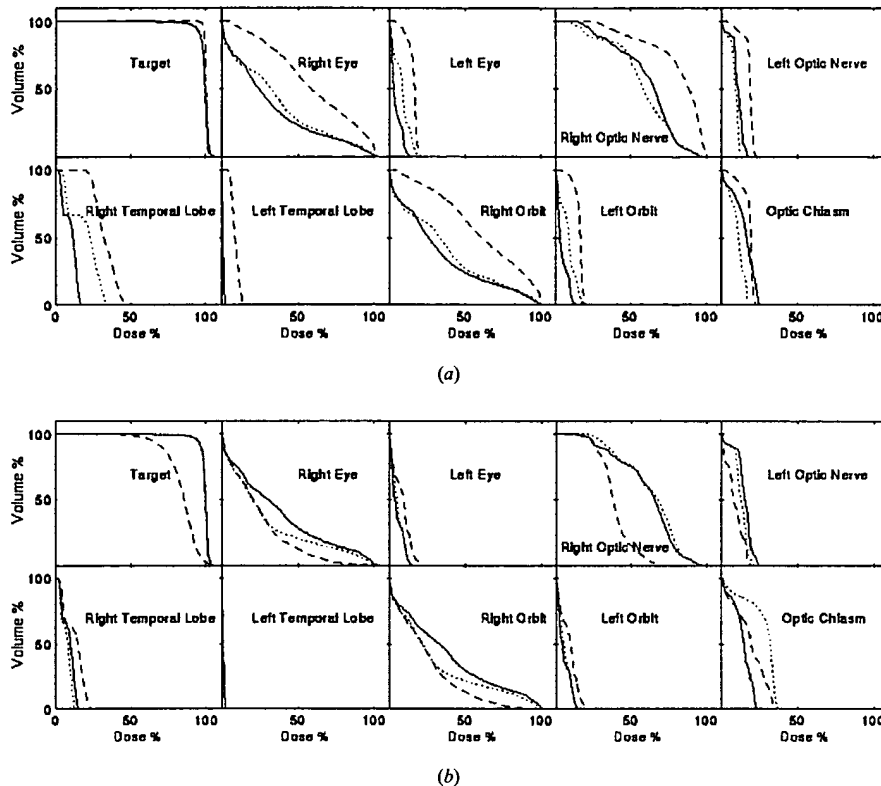


Figure 4. Systematic improvement of the DVHs with the iteration of the importance factors (IMs). The starting values of the IMs for figure 3(a) were unity for the target and zeros for all the sensitive structures. The dashed curves represent the corresponding initial 'optimal' DVHs. The dotted curves are the 'optimal' DVHs for a set of intermediate values of IMs (iteration #3). The optimal DVHs are plotted as full curves. The values of the IMs at different stages of the iteration are listed in table 1. Similar calculations were done by starting a different set of initial importance factors. The corresponding DVHs are plotted in figure 4(b). The initial, an intermediate and the final DVHs are shown as dashed, dotted and full curves. The corresponding values of the importance factors are shown in table 2.

were required for the score function to reach its minimum. The values of the importance factors corresponding to the initial (corresponding DVHs are shown as the dashed curves in figure 4(a)), intermediate (dotted curves in figure 4(a)), and the final state of the system (full curves in figure 4(a)) are shown in table 1. To see the change more clearly, we show the improvement of the isodose distributions on an axial and a sagittal plane in figures 5 and 6. The dose distributions shown in figure 5(a) and figure 6(a) correspond to the isodose plan obtained using the initial set of importance factors, and those shown in figures 5(b) and 6(b) are the final solution. The same solution was found when different sets of importance factors were used. In figure 4(b), the systematic improvement in the target and sensitive structure DVHs is plotted for a different set of initial set of importance factors. The values of the importance factors at different stages of the iterative calculation are tabulated in table 2. The solution showed similar behaviour as the importance factors were varied iteratively.

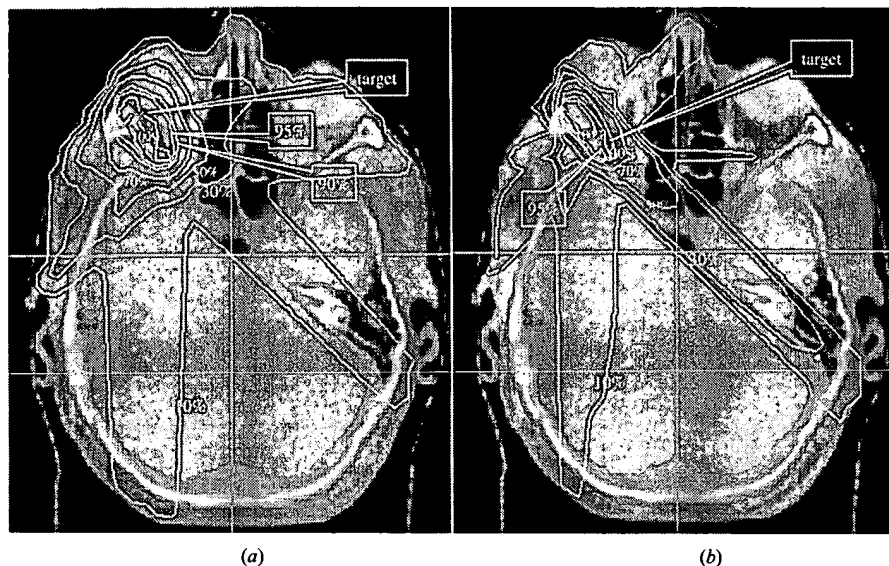


Figure 5. Axial isodose distributions corresponding to the initial set (a) and the final set of importance factors (b) for a four-field IMRT treatment of a lymphoma with the involvement of the right orbit.

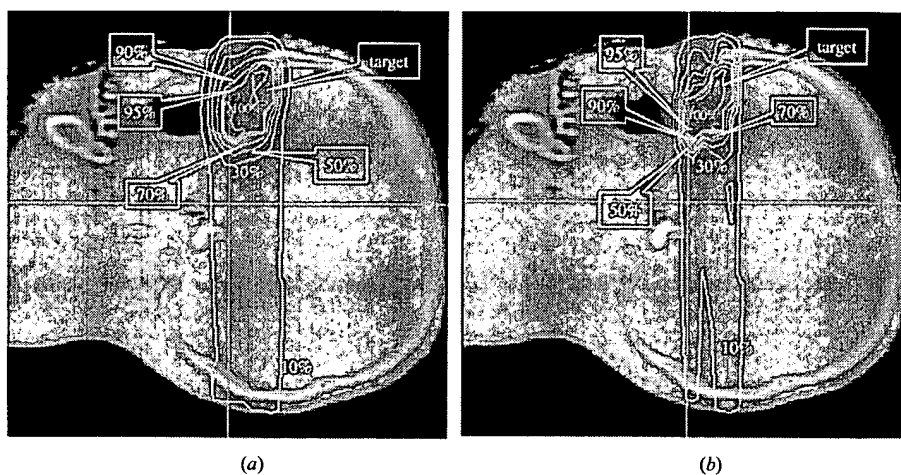


Figure 6. Sagittal isodose distributions corresponding to the initial set (a) and the final set of importance factors (b) for the same patient.

4. Summary

Inverse treatment planning is a multiobjective decision-making process in which there are conflicting clinical objectives. The trade-offs between the objectives for various anatomical structures can be parametrized by a set of importance factors. How to determine the importance

Table 1. The values of the importance factors at three different stages of the optimization for a four-field lymphoma treatment.

Iteration no	r_{target}	$r_{\text{right eye}}$	$r_{\text{left eye}}$	$r_{\text{right optic nerve}}$	$r_{\text{left optic nerve}}$	$r_{\text{right orbit}}$	$r_{\text{left orbit}}$	$r_{\text{right lens}}$	$r_{\text{left lens}}$	$r_{\text{optic chiasm}}$
Initial (iteration #1)	1	0	0	0	0	0	0	0	0	0
Intermediate (iteration #3)	1	0.92	0.11	0.39	0.08	0.03	0.01	0.03	0.09	0.46
Final (iteration #5)	1	0.96	0.28	0.08	0.14	0.02	0.08	0.81	0.42	0.26

Table 2. The values of the importance factors at three different stages of the optimization for a four-field lymphoma treatment with a different set of initial importance factors.

Iteration no	r_{target}	$r_{\text{right eye}}$	$r_{\text{left eye}}$	$r_{\text{right optic nerve}}$	$r_{\text{left optic nerve}}$	$r_{\text{right orbit}}$	$r_{\text{left orbit}}$	$r_{\text{right lens}}$	$r_{\text{left lens}}$	$r_{\text{optic chiasm}}$
Initial (iteration #1)	1	0.20	0.20	0.20	0.20	0.20	0.20	0.20	0.20	0.20
Intermediate (iteration #3)	1	0.92	0.05	0.06	0.01	0.04	0.06	0.97	0.21	0.08
Final (iteration #5)	1	0.96	0.28	0.07	0.12	0.02	0.07	0.82	0.42	0.25

factors efficiently is an important problem in the plan selection. In the past, little attention has been paid to this issue. In this paper, we have described an effective approach to determining the parameters. A decision rule or a score function is necessary in order to determine unambiguously the optimal importance factors. The response used to score the system can be based on experience, or simply an additional score function. A DVH based score function was introduced in our study to illustrate the methodology. Other types of score function based on, for example, biological models, can also be introduced for this purpose. An iterative algorithm for automatically selecting the importance factors was demonstrated. In the two-step optimization the trade-off strategy is specified in the DVH representation, and the final solution, which assimilates the specified relative importance of different structures, is found in the scheme of the quadratic objective function. This approach allows us to incorporate prior knowledge into the optimization process and to take advantage of the useful features of each scheme. The algorithm was applied to two clinical cases and the results indicated that the combined scheme of decision-making was effective and produced plans consistent with the planner's expectation. The approach has strong potential to automate the current trial-and-error IMRT treatment planning process and thus has widespread clinical implications.

Acknowledgments

The authors wish to thank R J Hamilton, D Spelbring, C A Pelizzari and G T Y Chen for their efforts during the development of SIITP. This work was supported in part by grant no IRG-58-008-40 from the American Cancer Society (ACS), a seed grant of the Radiological Society of North America (RSNA), a grant from Computerized Medical System (CMS) and grant no CA43840 awarded by the National Cancer Institute (NIH).

References

Brahme A, Roos J E and Lax I 1982 Solution of an integral equation encountered in rotation therapy *Phys. Med. Biol.* **27** 1221–9

Bortfeld T, Urkelbach J, Boesecke R and Schlegel W 1990 Methods of image reconstruction from projections applied to conformation therapy *Phys. Med. Biol.* **35** 1423–34

Carol M, Nash R H, Campbell R C, Huber R and Sternick E 1997 The development of a clinically intuitive approach to inverse planning: partial volume prescription and area cost function *Proc. 12th Int. Conf. on the Use of Computers in Radiation Therapy (Salt Lake City, Utah)* (Madison, WI: Medical Physics Publishing) pp 317–19

Ezzell G A 1996 Genetic and geometric optimization of three-dimensional radiation therapy *Med. Phys.* **23** 293–305

Holmes T W and Mackie T R 1994 A comparison of three inverse treatment planning algorithms *Phys. Med. Biol.* **39** 91–106

Ling C C, Chui C S, Jackson A, Kutcher G J, Leibel S, LoSasso T, Mohan R, Bortfeld T, Reinstein L, Spiro S, Wang X, Wu Q, Zelefsky M and Fuks Z 1996 Conformal radiation treatment of prostate cancer using inversely-planned intensity modulated photon beams produced with dynamic multileaf collimation *Int. J. Radiat. Oncol. Biol. Phys.* **35** 721–30

Lof J, Lind B K and Brahme A 1998 An adaptive control algorithm for optimization of intensity modulated radiotherapy considering uncertainties in beam profiles, patient set-up and internal organ motion *Phys. Med. Biol.* **43** 1605–28

Mohan R, Wang X, Jackson A, Bortfeld T, Boyer A L, Kutcher G J, Fuks Z and Ling C C 1994 The potential and limitations of inverse radiotherapy technique *Radiother. Oncol.* **32** 232–48

Olivera G H, Shepard D M, Reckwerdt P J, Ruchala K, Zachman J, Fitchard E E and Mackie T R 1998 Maximum likelihood as a common computational framework, in tomotherapy *Phys. Med. Biol.* **43** 3277–94

Press W H, Flannery B P, Teukolsky S A and Vetterling W T 1989 *Numerical Recipes in C* (New York: Cambridge University Press)

Starkschall G 1992 An iterative beam-weight optimization tool for three-dimensional radiotherapy treatment planning *Med. Phys.* **19** 155–63

Spiro S V and Chui C S 1998 A gradient inverse planning algorithm with dose-volume constraints *Med. Phys.* **25** 321–33

Togane D, Hamilton R J, Boyer A L and Xing L 1998 Dose volume histogram based optimization for intensity modulated radiation therapy *Med. Phys.* **25** A118

Webb S 1994 Optimizing the planning of intensity-modulated radiotherapy *Phys. Med. Biol.* **39** 2229–46

Xing L and Chen G T Y 1996 Iterative methods for inverse treatment planning *Phys. Med. Biol.* **41** 2107–23

Xing L, Hamilton R J, Pelizzari C A and Chen G T Y 1998a A 3D algorithm for optimizing beam weights and wedge filters *Med. Phys.* **25** 1858–65

Xing L, Hamilton R J, Spelbring D, Pelizzari C A, Chen G T Y and Boyer A 1998b Fast iterative algorithms for three-dimensional inverse treatment planning *Med. Phys.* **25** 1845–9

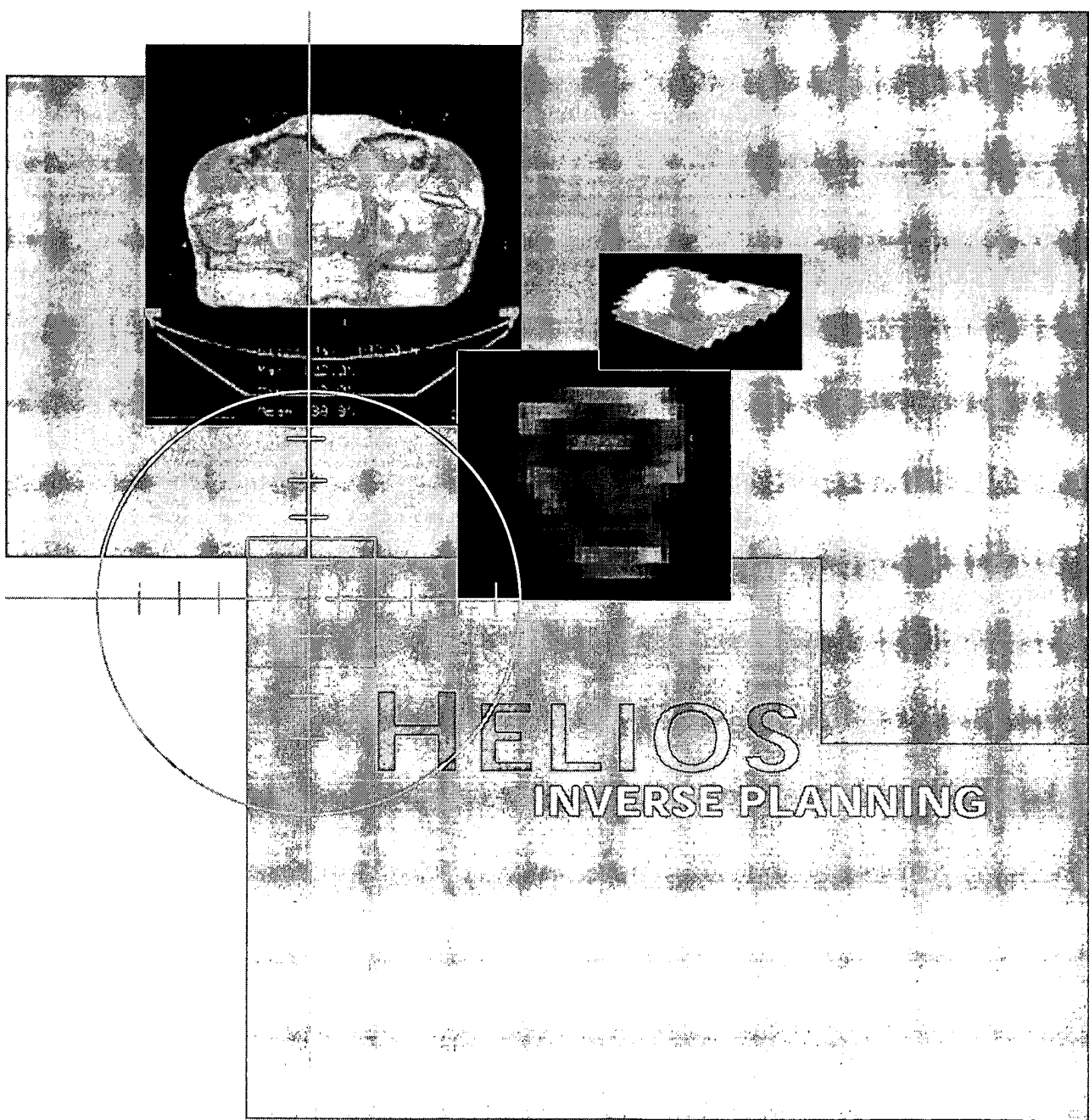
EXHIBIT

3

tables:

VARIAN
medical systems

ONCOLOGY
SYSTEMS



*Helios' Inverse planning module data works with
CadPlan PLUS' 2D treatment planning system. A completely
based graphical user interface that is friendly and direct for managing
RTs needs for the first time planners in its design and system.
Computer systems integration with the entire suite of CadPlan's Generation 6
products enable cost-effective configuration of a clinical IMRT program.*

Advanced INVERSE PLANNING

made easy



INTUITIVE

Inverse planning with Helios generates treatment plans with exquisite 3D dose conformity. In this prostate plan, the Planning Target Volume is completely covered by the prescribed Isodose line while dose to the rectum and bladder is minimized. Helios provides the key to improved patient outcome by permitting evaluation of the tumor dose while simultaneously reducing the dose delivered to critical organs.

INTEGRATED

Helios employs the same beam data and dose calculation algorithms already used in standard CadPlan PLUS 3D conformal treatment planning. Integration with CadPlan PLUS means no additional

EFFICIENT

The user can create a customized library of accepted dose optimization parameters that can be used in conjunction with the geometric plan libraries to maximize planning productivity.



HELIOS
PREPARATION
PLANNING
DELIVERY
SIMULATION
VERIFICATION

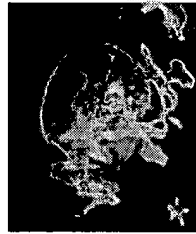
Inverse planning with Helios generates treatment plans with exquisite 3D dose conformity. In this prostate plan, the Planning Target Volume is completely covered by the prescribed Isodose line while dose to the rectum and bladder is minimized. Helios provides the key to improved patient outcome by permitting evaluation of the tumor dose while simultaneously reducing the dose delivered to critical organs.

Helios IMRT Process

Varian: The IMRT Technology Leader

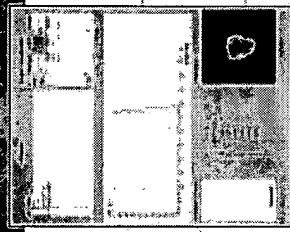
PROCESS DESIGN

Varian's distributed approach to treatment planning places functionality where it is needed most. The flexible design of the planning system supports many different clinical processes. The amount of contouring required for inverse treatment planning can increase significantly compared to conventional planning. In the distributed system, contouring and geometric planning may be performed on any SomaVision™ workstation within the department — including the physician's desktop computer — leaving the dose calculation engine free for intensive computation. Treatment plans may be evaluated in the dosimetry workspace before they are stored in the centralized VARIS™/Vision™ environment. Plans stored in the VARIS/Vision database share all of the clinical productivity benefits provided by full Generation 6 systems integration.

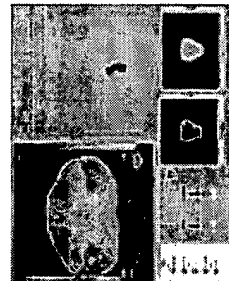


1

Geometric Planning: SomaVision
Targets and critical structures are contoured quickly with the advanced segmentation tools available in SomaVision. The physician may then enter a dose prescription and fractionation scheme and create the geometric treatment plan employing the powerful 3D visualization and virtual simulation tools in SomaVision.

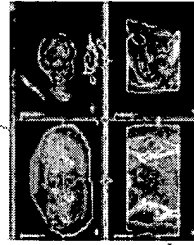


Dose Optimization: Helios
Helios automatically generates treatment plans that satisfy organ dose constraints provided by one physician. Helios' interactive user interface permits real-time adjustment of the dose optimization parameters by the physician, resulting in treatment plans that consistently outperform time-consuming and complex forward plans. The interactive user interface reduces the overall planning time and drastically shortens the learning curve associated with inverse planning.



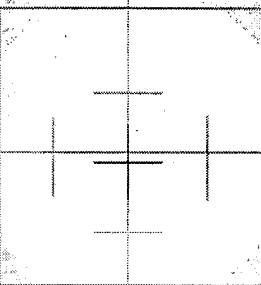
2

Dose Calculation: CoPlan PLUS
CoPlan PLUS employs a sophisticated Leaf Motion Calculator (LMC) to generate dynamic MultiLeaf Collimator (dMLC) treatment files appropriate for the user-selected delivery technique (Sliding Window, Multiple Static Segments, etc.). The final dose distribution is calculated according to the selected delivery technique to provide maximum correlation between the displayed and delivered dose.



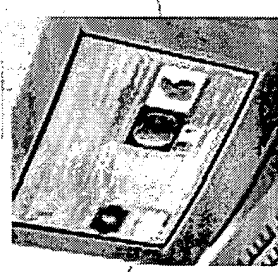
3

Dose Calculation: CoPlan PLUS
CoPlan PLUS employs a sophisticated Leaf Motion Calculator (LMC) to generate dynamic MultiLeaf Collimator (dMLC) treatment files appropriate for the user-selected delivery technique (Sliding Window, Multiple Static Segments, etc.). The final dose distribution is calculated according to the selected delivery technique to provide maximum correlation between the displayed and delivered dose.



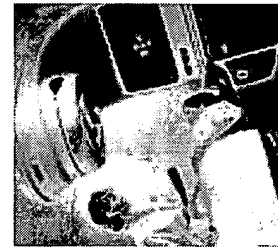
4

Plan Review: SomaVision
SomaVision provides powerful 3D dose visualization and analysis tools that make plan review possible anywhere! Comparison between Helios IMRT plans and standard conformal treatment plans is possible in SomaVision. After evaluation the physician may approve the plan electronically, automatically transferring the plan electronically to the VARIS database on the accelerator.



5

Information Management: VARIS
Helios IMRT treatments are stored in the VARIS database similar to any conventional treatment. VARIS can be used for charge capture and to generate detailed reports on IMRT treatments. Treatment planning parameters including DVH calculations are accessible for future outcomes analysis.



7

Verification: PortalVision™
PortalVision™ real time verification of patient positioning during IMRT treatments. With portal imaging the physicist may verify the accuracy of each delivered fluence matrix against those calculated.

6

Delivery: Clinac® with dMLC
The approved IMRT plan is automatically available for dynamic treatment on the Clinac. Integration of the treatment planning system and VARIS ensures that the correct field parameters and dMLC files are associated with the appropriate patient every time. Complete systems integration permits safe and rapid IMRT treatment delivery.

Dose OPTIMIZATION

DOSE OPTIMIZATION

This optimization module allows the delivery of intensity-modulated 3D dose distributions over multiple isocentres to reduce the dose delivered to normal tissue and increase the dose delivered to tumour. The inverse planning process begins with definition of the new objectives of the treatment plan. Given the reduced treatment time geometry, faster dose calculation times are required to produce dose distributions that closely conform to the user-specified dose prescription.

1.1.1

DOSE OPTIMIZATION

This optimization module allows the delivery of intensity-modulated 3D dose distributions over multiple isocentres to reduce the dose delivered to normal tissue and increase the dose delivered to tumour. The inverse planning process begins with definition of the new objectives of the treatment plan. Given the reduced treatment time geometry, faster dose calculation times are required to produce dose distributions that closely conform to the user-specified dose prescription.

1.1.2

DOSE OPTIMIZATION

This optimization module allows the delivery of intensity-modulated 3D dose distributions over multiple isocentres to reduce the dose delivered to normal tissue and increase the dose delivered to tumour. The inverse planning process begins with definition of the new objectives of the treatment plan. Given the reduced treatment time geometry, faster dose calculation times are required to produce dose distributions that closely conform to the user-specified dose prescription.

1.1.3

DOSE OPTIMIZATION

This optimization module allows the delivery of intensity-modulated 3D dose distributions over multiple isocentres to reduce the dose delivered to normal tissue and increase the dose delivered to tumour. The inverse planning process begins with definition of the new objectives of the treatment plan. Given the reduced treatment time geometry, faster dose calculation times are required to produce dose distributions that closely conform to the user-specified dose prescription.

1.1.4

DOSE OPTIMIZATION

This optimization module allows the delivery of intensity-modulated 3D dose distributions over multiple isocentres to reduce the dose delivered to normal tissue and increase the dose delivered to tumour. The inverse planning process begins with definition of the new objectives of the treatment plan. Given the reduced treatment time geometry, faster dose calculation times are required to produce dose distributions that closely conform to the user-specified dose prescription.

1.1.5

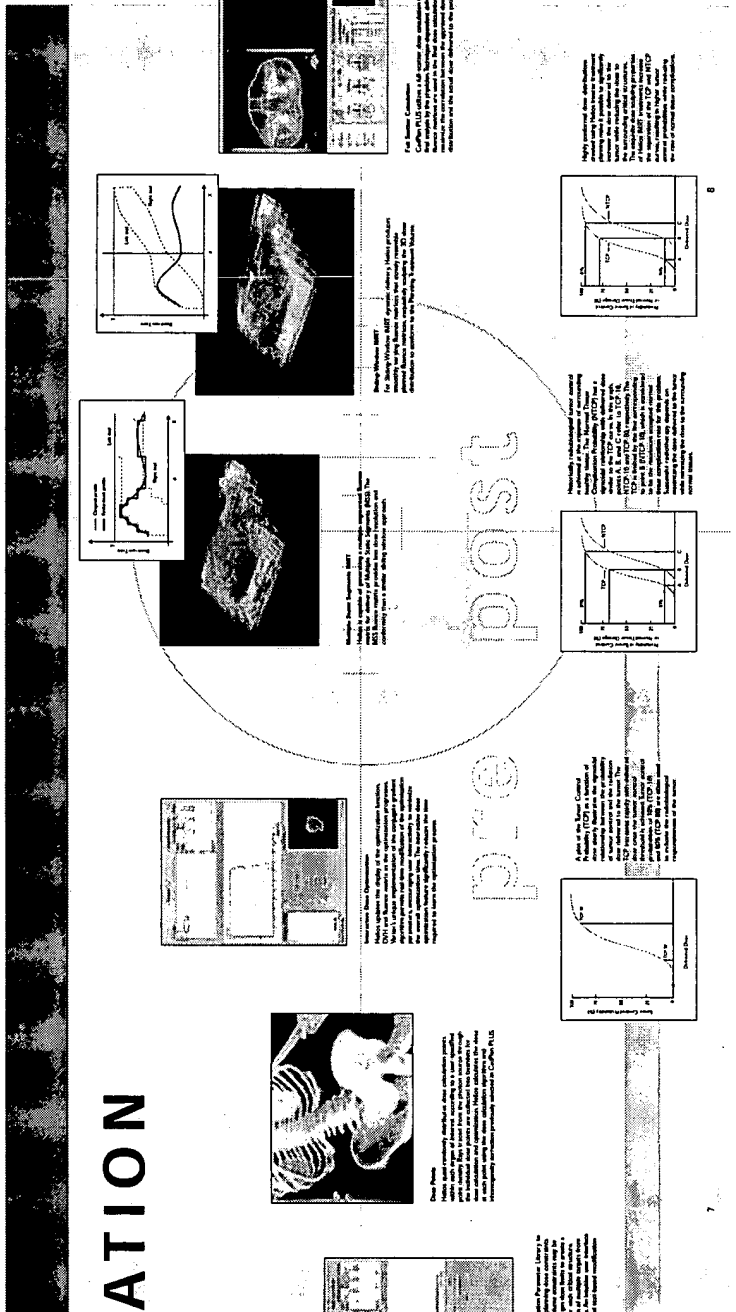
DOSE OPTIMIZATION

This optimization module allows the delivery of intensity-modulated 3D dose distributions over multiple isocentres to reduce the dose delivered to normal tissue and increase the dose delivered to tumour. The inverse planning process begins with definition of the new objectives of the treatment plan. Given the reduced treatment time geometry, faster dose calculation times are required to produce dose distributions that closely conform to the user-specified dose prescription.

1.1.6

DOSE OPTIMIZATION

This optimization module allows the delivery of intensity-modulated 3D dose distributions over multiple isocentres to reduce the dose delivered to normal tissue and increase the dose delivered to tumour. The inverse planning process begins with definition of the new objectives of the treatment plan. Given the reduced treatment time geometry, faster dose calculation times are required to produce dose distributions that closely conform to the user-specified dose prescription.



Conjugate Gradient Method

PURETETRACY

The conjugate gradient optimization method has been successfully implemented at our DOO (URF) University, China.

In addition, it has performed in international workshops including Europe, North America and Asia.

Optimization allows the clinician to specify the preferred dose and we do not have to choose a constraint for normal tissue and dose-volume constraints for normal tissue and critical structures. The conjugate gradient optimization algorithm is a parity unconstrained process independent of beam quality and geometry and therefore it is applicable to proton and electron beams in both single and multilevel beam treatments.

The conjugate gradient method generally affects the fluence method to quickly converge on the optimal dose distribution. The dynamic approach produces fluence entries that are directly correlated with the patient anatomy.

1.1.1

1.1.2

1.1.3

1.1.4

1.1.5

1.1.6

1.1.7

1.1.8

1.1.9

1.1.10

1.1.11

1.1.12

1.1.13

1.1.14

1.1.15

1.1.16

1.1.17

1.1.18

1.1.19

1.1.20

1.1.21

1.1.22

1.1.23

1.1.24

1.1.25

1.1.26

1.1.27

1.1.28

1.1.29

1.1.30

1.1.31

1.1.32

1.1.33

1.1.34

1.1.35

1.1.36

1.1.37

1.1.38

1.1.39

1.1.40

1.1.41

1.1.42

1.1.43

1.1.44

1.1.45

1.1.46

1.1.47

1.1.48

1.1.49

1.1.50

1.1.51

1.1.52

1.1.53

1.1.54

1.1.55

1.1.56

1.1.57

1.1.58

1.1.59

1.1.60

1.1.61

1.1.62

1.1.63

1.1.64

1.1.65

1.1.66

1.1.67

1.1.68

1.1.69

1.1.70

1.1.71

1.1.72

1.1.73

1.1.74

1.1.75

1.1.76

1.1.77

1.1.78

1.1.79

1.1.80

1.1.81

1.1.82

1.1.83

1.1.84

1.1.85

1.1.86

1.1.87

1.1.88

1.1.89

1.1.90

1.1.91

1.1.92

1.1.93

1.1.94

1.1.95

1.1.96

1.1.97

1.1.98

1.1.99

1.1.100

1.1.101

1.1.102

1.1.103

1.1.104

1.1.105

1.1.106

1.1.107

1.1.108

1.1.109

1.1.110

1.1.111

1.1.112

1.1.113

1.1.114

1.1.115

1.1.116

1.1.117

1.1.118

1.1.119

1.1.120

1.1.121

1.1.122

1.1.123

1.1.124

1.1.125

1.1.126

1.1.127

1.1.128

1.1.129

1.1.130

1.1.131

1.1.132

1.1.133

1.1.134

1.1.135

1.1.136

1.1.137

1.1.138

1.1.139

1.1.140

1.1.141

1.1.142

1.1.143

1.1.144

1.1.145

1.1.146

1.1.147

1.1.148

1.1.149

1.1.150

1.1.151

1.1.152

1.1.153

1.1.154

1.1.155

1.1.156

1.1.157

1.1.158

1.1.159

1.1.160

1.1.161

1.1.162

1.1.163

1.1.164

1.1.165

1.1.166

1.1.167

1.1.168

1.1.169

1.1.170

1.1.171

1.1.172

1.1.173

1.1.174

1.1.175

1.1.176

1.1.177

1.1.178

1.1.179

1.1.180

1.1.181

1.1.182

1.1.183

1.1.184

1.1.185

1.1.186

1.1.187

1.1.188

1.1.189

1.1.190

1.1.191

1.1.192

1.1.193

1.1.194

1.1.195

1.1.196

1.1.197

1.1.198

1.1.199

1.1.200

1.1.201

1.1.202

1.1.203

1.1.204

1.1.205

1.1.206

1.1.207

1.1.208

1.1.209

1.1.210

1.1.211

1.1.212

1.1.213

1.1.214

1.1.215

1.1.216

1.1.217

1.1.218

1.1.219

1.1.220

1.1.221

1.1.222

1.1.223

1.1.224

1.1.225

1.1.226

1.1.227

1.1.228

1.1.229

1.1.230

1.1.231

1.1.232

1.1.233

1.1.234

1.1.235

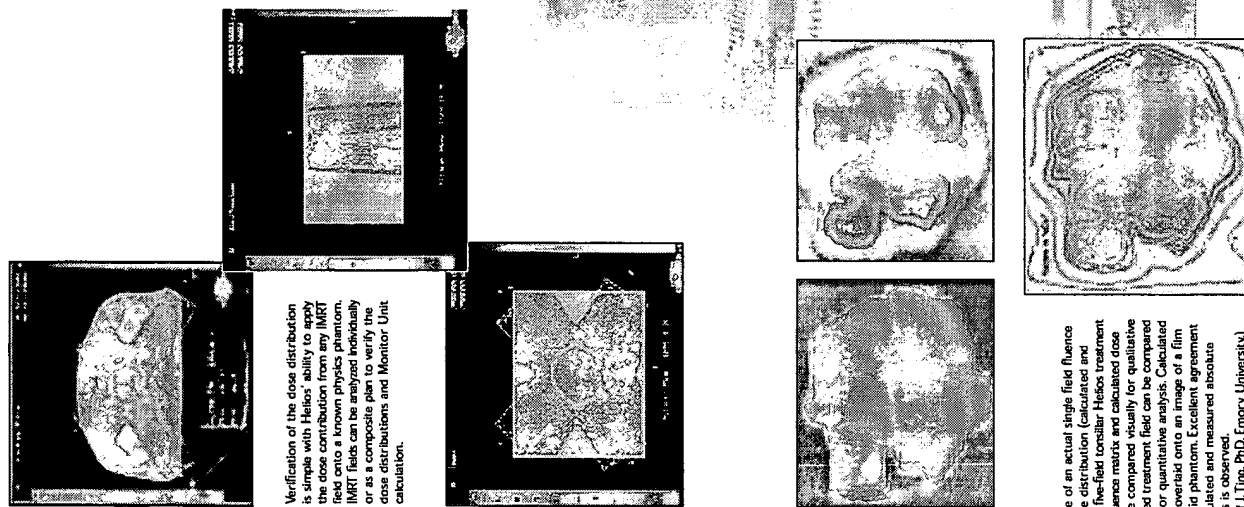
Plan Verification

QUALITY ASSURANCE

Plan verification is simplified using powerful physics tools incorporated in the Helios IMRT package. Helios calculates the final dose distribution using fluence matrices corresponding to the user selected delivery technique. A dMLC Visualizer simulates the MLC motion as a function of the delivered dose, and permits visual comparison of the deliverable fluence to the optimal fluence by the physicist. Export of the fluence matrices for comparison with film measurement is easily accomplished with the Helios IMRT system.

Any fluence matrix may be applied to a known physics phantom for verification of the dose distribution and Monitor Unit calculation. Either a single field or a composite plan consisting of all treatment beams can be calculated for verification of dose distributions. The user can extract 2D dose distributions in any arbitrary plane for direct comparison with film measurement. Verifying the delivered fluence distribution with PortalVision completes the comprehensive set of quality assurance tools to provide confirmation of accurate clinical treatments.

This is an example of an actual single field fluence and resultant dose distribution (calculated and measured) from a five-field tonsil Helios treatment plan. The actual fluence matrix and calculated dose distribution can be compared visually for qualitative analysis. The planned treatment field can be compared to measurement for quantitative analysis. Calculated isodose lines are overlaid onto an image of a film irradiated in a solid phantom. Excellent agreement between the calculated and measured absolute dose distributions is observed.
(Data courtesy of L.Ting, PhD, Emory University)



Varian is the IMRT technology leader.
Years of innovation have created the depth and breadth necessary to revolutionize the complex challenges of IMRT. Complexity and productivity are key elements. From the design of our products and architecture to the unique environment. From depth-of-field planning to quality assurance tools for fine-tuning the different types of plans and treatments. In the future, innovation will continue in conjunction with the CadPlan PLUS 3D treatment planning system, providing a step forward towards more intelligent IMRT planning. By offering both Varian's static Segmented and dynamic Segmented IMRT delivery systems, Helios provides the ultimate in complete control of the IMRT process. The key to better patient outcomes is to select the tool to perform the volume and intensity directly surrounding critical structures—achievable now with Helios.

Quality assurance tools and complete systems integration provide fast and safe IMRT implementation.



Oncology Systems
3100 Hansen Way
Palo Alto, CA 94304-1038
tel 650.424.5700
tel 800.544.4636
www.varian.com

VARIAN MEDICAL SYSTEMS WORLDWIDE OFFICES

USA Headquarters

California
Varian Medical Systems
Palo Alto, CA 94304
Tel 650.424.5700
800.544.4636
Fax 650.424.5437
<http://www.varian.com>

USA Regional Offices

California
Varian Medical Systems
Corona, CA
Tel 909.280.4401
Fax 909.280.4300

Georgia
Varian Medical Systems
Marietta, GA
Tel 770.955.0367
Fax 770.955.6918

Illinois
Varian Medical Systems
Deer Park, IL
Tel 847.449.5533
Fax 847.449.0443

Tennessee
Varian Medical Systems
Franklin, TN
Tel 615.793.7165
Fax 615.793.2749

International Sales Offices

Australia
Varian Medical Systems
(Australia) Pty Ltd
Parramatta,
NSW 2153

Austria
Varian Medical Systems
Zug, Switzerland

Eastern Europe
Varian Medical Systems
International AG
Zug, Switzerland

Africa, Middle & Near East
Varian Medical Systems
Netherlands

France
Varian Medical Systems
Paris, France

Belgium & Netherlands
Varian Medical Systems
Netherlands

Brazil
Varian Medical Systems
do Brasil Ltda
Sao Paulo, Brazil
Tel 55.11.5236.7053
Fax 55.11.5245.0748

China

Varian Medical Systems
China Ltd.
Beijing, PR China
Tel 8610.65127169
Fax 8610.65132089

Finland
Varian Medical Systems
Helsinki

Latvia
Varian Medical Systems
Riga

Germany
Varian Medical Systems
Darmstadt, Germany
Tel 49.6151.75160
Fax 49.6151.751618

Japan
Varian Medical Systems
Tokyo, Japan
Tel 81.3.5545.7070
Fax 81.3.5545.5223

Hong Kong

Varian Medical Systems
Pacific Inc.
Kowloon, Hong Kong
Tel 852.2724.2336
Fax 852.2730.1280

India
Varian Medical Systems
Mumbai

Italy
Varian Medical Systems
Italy, S.p.A.

Ireland
Varian Medical Systems
Cork, Ireland

Spain/Portugal
Varian Medical Systems
Barcelona, Spain

UK/Ireland
Varian Medical Systems
UK Ltd.

Scandinavia
Varian Medical Systems
Stockholm, Sweden

Merica, Denmark
Tel 354.650.1000
Fax 354.650.930

Latin America

Varian Medical Systems
Miami, FL USA
Tel 305.261.7666
Fax 305.266.7770

Spain/Portugal
Varian Medical Systems
Barcelona, Spain

Merica, Spain
Tel 343.759.4530
Fax 343.759.4541

UK/Ireland
Varian Medical Systems
UK Ltd.

Canada, West, Mexico
Tel 416.299.4312-24
Fax 416.299.5700

Reprinted from the *ACR Bulletin*, April 2001, Volume 57, Issue 4, pp. 4-5, 10:

New Intensity-modulated Radiation Therapy Codes for Hospital Outpatient Procedures

The Health Care Financing Administration (HCFA) has designated two new interim codes that cover the work effort and equipment cost for planning and delivery of intensity-modulated radiation therapy (IMRT). These temporary "G" codes may only be billed in the hospital outpatient setting. They do not apply to physician offices or freestanding centers. This article discusses the two new codes and provides general guidance to ACR and ASTRO members about IMRT, from the ACR/ASTRO Joint Economics Committee (JEC), on their application in the hospital outpatient setting only. It does not and is not intended to provide guidance on or express an opinion with respect to IMRT planning and delivery in the physician office or freestanding clinic settings. HCFA defines the following interim codes and descriptors:

G0174 – Intensity-modulated radiation therapy (IMRT) delivery to one or more treatment areas, multiple couch angles/fields/arcs, custom-collimated pencil-beams with treatment setup and verification images, complete course of therapy requiring more than one session, per session.

G0178 – Intensity-modulated radiation therapy (IMRT) plan, including dose-volume histograms for target and critical structure partial tolerances, inverse plan optimization performed for highly conformal distributions, plan positional accuracy and dose verification, per course of treatment.

Both of the new codes have been assigned to APC 0302 Level III Radiation Therapy with a payment rate for Medicare beneficiaries of \$407.18. These codes were approved by HCFA for use in implementing the Ambulatory Payment Classifications under the Hospital Outpatient Prospective Payment System and were effective Jan. 1. As such, they are only to be used to reimburse the technical effort (Medicare Part A) in the hospital outpatient implementation of IMRT. Physician work effort continues to be reimbursed under the current Physician Fee Schedule (Medicare Part B) in the hospital environment.

At this juncture, other existing CPT codes are to be used to cover IMRT work effort performed in offices or stand-alone clinics, because a CPT equivalent to the G0174 or G0178 codes does not exist.

The AMA's CPT Editorial Panel has accepted ACR/ASTRO-recommended definitions for IMRT planning (773xx) and IMRT delivery (774xx) codes. These codes are now being sent to the AMA's Relative Value Update Committee (RUC) for valuation. If the values are approved this spring, it is anticipated that HCFA and private insurance carriers will have codes available for reimbursement of technical services in freestanding centers and for professional services in all practice locales by Jan. 1, 2002.

IMRT planning and delivery is a new approach for obtaining the highly conformal dose distributions needed to irradiate complex targets positioned near or invaginated by sensitive normal tissues. Treatment planning for IMRT is different than conventional 3-D conformal radiation therapy in that the starting point is a description of the desired dose distribution rather than the application of traditional fields and beam modifiers to generate an acceptable plan. The new technique, commonly called inverse planning, was first proposed by Andres Brahme in 1988 and formally defined as a computer optimization process that develops a dose distribution based on the input of specific dose constraints for the target(s) and nearby critical structures.¹ These regions of interest must be identified by a contouring procedure, and the optimization must sample the dose with a grid spacing of 1 centimeter or less.

IMRT dose delivery must use a multileaf collimator (MLC) with leaves that project to a nominal 1 cm or less at the treatment unit isocenter. The exact delivery method is not restricted as long as the particular technique chosen has the ability to model the highly modulated intensity patterns that result from the planning process described above. However, the use of an MLC to produce simple one-dimensional ramp intensity distributions is excluded because the inverse planning process is not expected to produce these intensity patterns.

In order to use these billing codes, dose reporting must include dose-volume histograms for all targets and critical structures, and representative dose distributions that characterize the 3-D dose distribution. Because IMRT dose distributions are intended to be highly conformal, verification of the field placement is extremely important.

Immobilization must be considered as an essential part of the IMRT process, and ***reporting must include documentation of field positioning relative to the patient's anatomy as viewed with an appropriate imaging study. Additionally, the accuracy of dose delivery must be documented for each course of treatment by irradiating a phantom that contains either calibrated film to sample the dose distribution or an equivalent measurement system to verify that the dose delivered is the dose planned.**** The dosimetry should be verified using an ionization chamber.

Code Utilization

- Code G0174 may be charged once per session for any fixed-gantry dose delivery technique that uses an MLC system that automatically sequences field shapes and corresponding monitor unit settings. This delivery can be either dynamic or step-and-shoot. Dynamic delivery is defined as changing field shapes with the X-ray beam on. Sliding-window delivery is a step-and-shoot technique that simulates dynamic treatment by moving between control points with the beam turned off. The use of superimposed-field segments is another step-and-shoot method that changes field shapes during irradiation pauses. For either step-and-shoot method, an average of at least four segments per gantry angle must be used to justify billing under code G0174.
- Code G0174 may be charged once per session for IMRT techniques that use a rotating-gantry dose-delivery technique with changing field shape as the gantry moves. A

* Emphasis added by Radiological Imaging Technology, Inc.

single sweep of the gantry with the field conforming to the outer boundaries of the target is not considered to be IMRT.

- Dose delivery with a physical compensator does not currently justify the use of code G0174 in the opinion of the JEC, based on HCFA's definition of this code. Future demonstration of equivalent efficacy for compensator-based IMRT would require separate consideration for coding in the future.
- Code G0174 can only be used in situations where the plan being implemented meets the description of code G0178 and the definition of inverse planning given above.
- The technical reimbursement within CPT code 77470 [Special treatment procedure (e.g., total body irradiation, hemibody radiation, per oral, endocavitary or intraoperative cone irradiation)] is not incorporated in G0174 and may be charged separately.
- Code G0178 may be charged for inverse treatment planning once per treatment course. Treatment of a number of separate metastases in the brain must be considered as a single planning task, and code G0178 can be used only one time.
- Code G0178 precludes billing for the technical component of CPT 77295 (Therapeutic radiology simulation-aided field setting; three-dimensional) and its inclusions (see the article on CPT code 77295 in the November 2000 issue of the *ACR Bulletin*).
- Patient position verification per session may be charged to code CPT 77417 [Therapeutic radiology port film(s)] per existing Carrier Medical Director policy for use of this code.
- Technical component billing for the following codes is incorporated in G0178 and should not be charged separately: 77305 [(Teletherapy, isodose plan (whether hand- or computer-calculated); simple (one or two parallel opposed unmodified ports directed to a single area of interest)], 77310 [Teletherapy, isodose plan (whether hand- or computer-calculated); intermediate (three or more treatment ports directed to a single area of interest)], 77315 [Teletherapy, isodose plan (whether hand- or computer-calculated); complex (mantle or inverted Y, tangential ports, the use of wedges, compensators, complex blocking, rotational beam or special beam considerations)], and 77321 (Special teletherapy port plan, particles, hemibody, total body).

Documentation

The following documentation must be provided:

- For G0174 – Permanent records of daily treatment delivery for each field, including the date, treatment unit settings and dose delivered; verification images and MLC sequence for each field; and evidence of physician review for each treatment course.

- For G0178 – Permanent records of computer-generated inverse treatment plans, including 3-D tumor and critical structure volumes, inverse planning dosimetric or biological objectives, dose-volume histograms and dose verification; and evidence of physician review.

Medical Necessity

IMRT planning and delivery are clinically warranted when one or more of the following conditions exist:

- The target volume is irregularly shaped and in close proximity to critical structures that must be protected.
- IMRT is the only option to cover the volume of interest with narrow margins and to protect immediately adjacent structures.
- An immediately adjacent area has been previously irradiated, and abutting portals must be established with high precision.
- IMRT is the only option when additional precautions for reducing the GTV, CTV or PTV margins, such as gating delivery, are used.
- Only IMRT can produce dose distributions that can cover extremely concave target geometries.

If you have any questions or need further information, please call the economics and health policy department at (800) 227-5463, ext. 4923.

Reference

1. Brahme A. Optimization of stationary and moving beam radiation techniques. Radiother and Oncol. 1988;12:(2):129-40.

IMRT Error in the 2001 HCPCS Book

Errors for IMRT codes G0174 and G0178 have been identified in the 2001 Health Care Financing Administration Common Procedure Coding System (HCPCS) book. Specifically, the HCPCS descriptors have been incorrectly inverted to state G0174 as the plan code and G0178 as the delivery code for IMRT. The two IMRT "G" code descriptors should state G0174 as the delivery code and G0178 as the plan code. If you have questions regarding this update, call the ACR's economics and health policy department at (800) 227-5463, ext. 4923.

Reprinted with permission of the American College of Radiology, Reston, Virginia. No other representation of this material is authorized without express, written permission from the American College of Radiology.